High Accuracy Correction of Blackbody Radiation Shift in an Optical Lattice Clock

Thomas Middelmann, Stephan Falke,* Christian Lisdat, and Uwe Sterr
Physikalisch-Technische Bundesanstalt (PTB), Bundesallee 100, 38116 Braunschweig, Germany
(Received 14 August 2012; published 27 December 2012)

We have determined the frequency shift that blackbody radiation is inducing on the $5s^2\ {}^1S_0$–$5s5p\ {}^3P_0$ clock transition in strontium. Previously its uncertainty limited the uncertainty of strontium lattice clocks to 1×10^{-16}. Now the uncertainty associated with the blackbody radiation shift correction translates to a 5×10^{-18} relative frequency uncertainty at room temperature. Our evaluation is based on a measurement of the differential dc polarizability of the two clock states and on a modeling of the dynamic contribution using this value and experimental data for other atomic properties.

DOI: 10.1103/PhysRevLett.109.263004 PACS numbers: 32.10.Dk, 06.20.F−, 32.60.+i, 44.40.+a

The performance of optical clocks promises a large variety of benefits. Ultimately the definition of the SI unit for time and frequency could be reworded to exchange the microwave transition as reference by an optical one. At present, the realization of the second would be improved in accuracy by more than an order of magnitude [1]; its stability could be increased even by several orders of magnitude [2–4]. Even without a change in definition, because of their accuracy optical clocks serve to probe the Universe in real time for temporal variations of the fundamental constants [1,5,6] like the fine structure constant α or coupling of fundamental constants to forces like, e.g., gravity [7]. In combination with their outstanding stability, they are also considered to be the key instruments that could enable new measurement opportunities like relativistic geodesy [8,9] with high temporal resolution as a supplement to established gravimetric techniques by comparing gravitational potentials directly.

In the quest for the best clocks, lattice clocks offer the highest stability [2–4] but suffer from blackbody radiation (BBR) shifts [10–12]. Among these, strontium clocks are pursued in several experiments worldwide [10,11,13,14]. Their systematic uncertainty now reaches the 1×10^{-16} level and is thus significantly below that of primary frequency standards used for frequency measurements. The correction for the shift by the blackbody radiation typically dominates the uncertainty budget of the strontium clocks. Besides uncertainty due to the temperature measurement, at present the uncertainty of the atomic response to BBR at room temperature contributes 7×10^{-17} to the uncertainty. The obvious strategy to improve clock accuracy by reducing the environmental temperature requires involved apparatuses. Instead, in most clocks accurate corrections of the BBR shift are applied. This correction is so far only known from atomic structure calculations [15,16] and lacks experimental verification.

As the frequency of room temperature BBR is very low, measurements of the difference of the dc polarizabilities of the two clock states greatly improves the knowledge about the BBR shift. In the case of an optical frequency standard with neutral ytterbium, recent experiments demonstrated a significant reduction of uncertainty of the BBR shift correction by measuring the frequency sensitivity of the clock transition to a dc electric field [12]. Similar approaches have been pursued for Cs clocks [17,18].

However, in both strontium and ytterbium, more than the differential static polarizability $\Delta\alpha$ needs to be considered at the level of 10^{-16} relative frequency uncertainty due to low-frequency lines (Fig. 1). In the BBR shift a dynamical correction $\Delta\nu_{\mathrm{dyn}}(T)$ has to be applied [15]:

$$\Delta\nu_{\mathrm{BBR}} = -\frac{1}{2h}\Delta\alpha\langle E^2\rangle_T + \Delta\nu_{\mathrm{dyn}}(T), \tag{1}$$

where $\langle E^2\rangle_T \approx (8.319\ \mathrm{V/cm})^2 \times (T/300\ \mathrm{K})^4$ is the mean squared electric field of the BBR radiation of temperature T. To first order, $\Delta\nu_{\mathrm{dyn}}(T)$ scales with T^6. In the case of strontium it contributes to the relative frequency shift due to BBR at a level of 3×10^{-16} [15,16].

In this work we reduce the uncertainty of the BBR frequency shift coefficient of the 429 THz $(5s5p)^3P_0$–$(5s^2)^1S_0$ clock transition of Sr in two steps: first, through a measurement of the differential dc polarizability $\Delta\alpha$ to provide a high

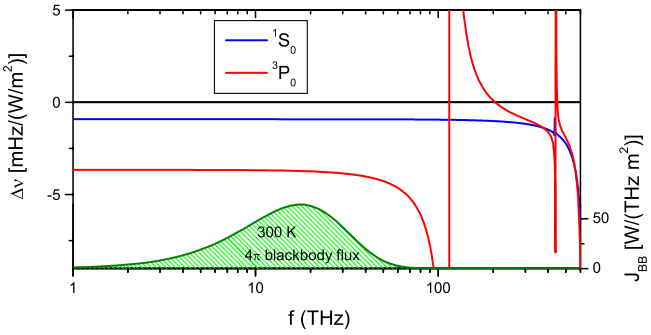

FIG. 1 (color online). ac polarizabilty of the two clock states ${}^1S_0$ and ${}^3P_0$ as a function of the frequency and room temperature blackbody spectrum J_{BBR}. The resonance structure in the ${}^3P_0$ polarizability is due to 115 THz $5s4d\ {}^3D_1$–${}^3P_0$ transition. The magic wavelength lattice is at the crossing of both ac polarizability curves at 369 THz.

precision experimental value for the largest fraction of the shift, and second, we use this observable along with several others to model the dynamic BBR shift, i.e., $\Delta\nu_{\mathrm{dyn}}$. From the improved model of the response to BBR, the current leading contribution to the uncertainty of Sr clocks can now be reduced by an order of magnitude to 5×10^{-18} at room temperature.

To measure $\Delta\alpha$ we equipped our strontium lattice clock apparatus with a precision capacitor and a moving optical lattice setup [19] to transfer atoms from the loading to the interrogation region. Samples of few 10^4 ^{88}Sr atoms at around 2 μK are created by Zeeman slowing and laser cooling in a two-stage magneto-optical trap [20] and trapped in the horizontal one-dimensional lattice with a waist radius of 65 μm and trap frequencies of 70 kHz axial and 200 Hz radial at a trap depth of 9 μK.

To maintain the trap depth throughout the transport of atoms over several Rayleigh ranges of the focused lattice beams, the waist of the lattice beams is moved together with the interference pattern. This is achieved by moving the beam shaping optics and retroreflection unit with translation stages. This setup allows us to move the atoms from the magneto-optical trap region into the capacitor and, after interrogation by the clock laser, back out for detection by laser induced fluorescence on the $(5s5p)^1P_1$–$(5s^2)^1S_0$ transition. We also detect the atom number in the $^3P_0$ state by repumping them to the $^1S_0$ state to reduce atom number fluctuation related noise. To avoid a first order Doppler shift during the interrogation of the clock transition due to residual motion of the stages, we stabilize the path length between clock laser and atom position represented by the retroreflection mirror of the lattice [21].

The capacitor consists of two Zerodur plates, separated by two optically contacted Zerodur gauge blocks of 5 mm height (see Fig. 2), that were determined interferometrically using three wavelengths [22]. The plates are partially coated with semitransparent gold layers (20 nm) and underlying contact layers of aluminum (5 nm) to allow for an interferometric determination of the electrode separation before installation. The measured surface flatness of the plates leads to a correction of $-153(28)$ nm (Table I) at the position of the atoms. Here, we observe locally an angle between the electrodes of 5 μrad, which corresponds to the measured parallelism of the gauge blocks' surfaces and the flatness of the electrode plates. After assembling the capacitor the field plate separation was confirmed by an independent direct interferometric measurement. As the plate separation was measured before the capacitor was brought into the vacuum chamber, we also include contributions as relaxation under vacuum, bending the plates under the influence of gravity or thermal expansion. The conductive surface of 28 mm $\times$ 67 mm ensures field homogeneity of better than 10^{-6} over a large area (Fig. 2).

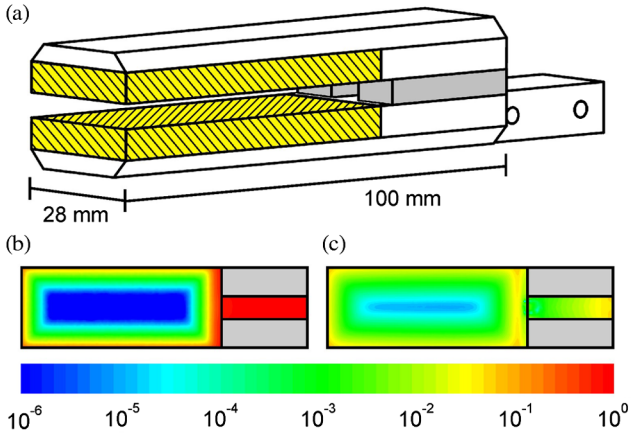

FIG. 2 (color online). Precision capacitor. (a) A sketch to scale. The hatched areas depict the gold plated electrodes. (b) Deviation of the electric field from an infinite capacitor with U/d, when voltages $\pm U/2$ are applied. (c) z component of the stray field $\vec{E}_0$ leaking into the capacitor on a plane 1 mm above the center when both electrodes are on the potential $U/2$. Both fields from finite element calculations are normalized to U/d.

Voltage is supplied to both electrodes by two electric wires, each connected to the electrodes at points with maximum separation to also allow for measurements of residual resistance of the connections. Independent voltages of up to 700 V can be applied to the electrodes from two precision voltage supplies (Fluke 415B). The voltage difference is monitored by a precision voltmeter (HP 3458A calibrated via a Fluke 5720A calibrator to a Josephson voltage standard), with an averaging time of 1000 power line cycles (50 Hz). The electrodes are connected to the voltage supplies with reed relays, which allow for inverting or discharging the capacitor without interrupting the voltage measurement.

We measure the field induced shift of the atomic resonance in ^{88}Sr in three field configurations (applied field, inverted field, and no field) by interleaving three stabilizations [11,23] of the clock laser to the atoms. Information on the shift induced by the capacitor $\vec{E}_{\mathrm{cap}}$ and small bias fields $\vec{E}_0$ is

TABLE I. Uncertainty budget for the capacitor plate separation.

Source	Correction (nm)	Uncertainty (nm)
Gauge block height	-	11.3
Contacting	0	11.3
Coating	-50	15
Parallelism	-153.1	27.7
Position	0	10
Bending of plates	0	13.1
Electrostatic forces	0	0.04
Compression by air pressure	2.8	0.1
Temperature gauge blocks	0	2.5
Temperature field plates	0	6.0
Separation	5 001 644.2	39.5

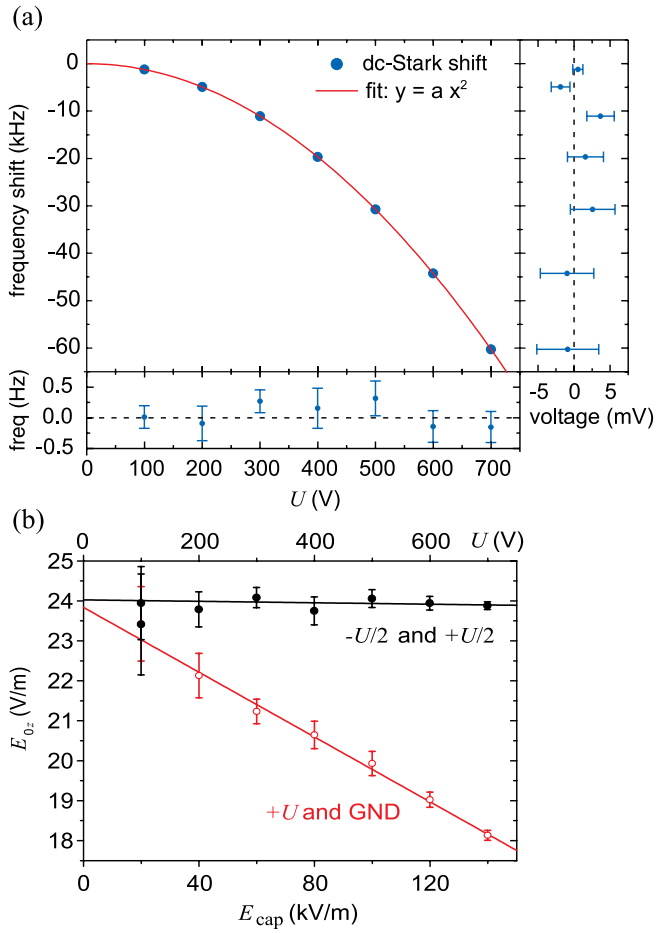

FIG. 3 (color online). Measured differential dc-Stark shift. (a) Measured data and a fitted parabola along with the residuals. (b) Measured bias field component in the z direction. GND, ground potential.

contained in the three offset frequencies ν_i ($i = \uparrow, \downarrow, 0$) to the reference cavity of the clock laser.

As the observed shift is proportional to $(\vec{E}_{\mathrm{cap}} + \vec{E}_0)^2$, the dc-Stark shift due to $\vec{E}_{\mathrm{cap}}$ alone is given by

$$\nu_{\mathrm{dc}} = (\nu_\uparrow + \nu_\downarrow)/2 - \nu_0, \tag{2}$$

provided changes in $\vec{E}_0$ are slow compared to the cycle times. The data of a typical experimental run are shown in Fig. 3 with residuals from a parabolic fit.

The component of a small bias field E_{0z} along the direction of the applied field $\vec{E}_{\mathrm{cap}}$ is given by

$$\nu_\uparrow - \nu_\downarrow \propto \vec{E}_{\mathrm{cap}} \cdot \vec{E}_0 = E_{\mathrm{cap}} E_{0z}. \tag{3}$$

The bias field E_{0z} can be explained as the sum of patch fields independent of the applied field and stray fields. Patch fields can occur, e.g., due to a difference in the work function of the gold coatings, which depends on the crystalline structure and can have a magnitude of up to 500 meV [24,25]. They explain the part of E_{0z} that is independent of the applied voltage (Fig. 3). However, differences in the work function do not explain the voltage dependence of E_{0z}. As this behavior may indicate residual differences between the voltage of the capacitor and the measured voltage, it was crucial to understand it: The system can be described by three electrodes (two capacitor electrodes at potentials U_1 and U_2 and the surrounding vacuum system on ground potential). Any field in this model can be written as the sum of the antisymmetric configuration with electrodes at $\pm(U_1 - U_2)/2$ and a stray field with both electrodes at the average potential $(U_1 + U_2)/2$. This stray field $\propto U_1 + U_2$ is contributing to E_{0z} if the atoms are not probed exactly on the symmetry axis of the capacitor [Fig. 2(c)]. Simulations confirm that an offset of 1 mm above the capacitor's symmetry plane with a shift of 1 mm to one side explains the observed dependence on the applied voltage, which is compatible with our effort on positioning.

This stray field explains the voltage dependence of E_{0z}, and thus Eq. (2) can be applied to determine ν_{dc} (neglecting an insignificant quadratic contribution from $\vec{E}_0$). No significant time dependence of E_{0z} is observed. Along with measured discharging curves of the electrodes and measurements of the resistance of the capacitor plates against ground potential and between feed lines to one plate, we conclude that the measured voltage U determines $E_{\mathrm{cap}} = U/d$.

Several parabolas as in Fig. 3(a) were measured and $\Delta\alpha$ was derived for each voltage. We confirmed that neither alternating the order of the three interrogations nor adding a second zero field cycle caused any systematic effect. No significant day-to-day variation of $\Delta\alpha$ was observed. To properly account for different uncertainty contributions of the voltmeter, we first averaged the $\Delta\alpha$ values for each applied voltage. In a second step all these values were averaged with weights according to the uncertainty. We obtain the differential dc polarizability $\Delta\alpha = 4.07873(11) \times 10^{-39}\ \mathrm{C\,m^2/V}$. An influence of the hyperpolarizability scaling with E^4 was investigated by fitting a parabola of type $a + bE^2$ to the $\Delta\alpha$ obtained in the first averaging step. The difference between a and the weighted average of $\Delta\alpha$ was taken as the uncertainty contribution for the hyperpolarizability. A complete list of uncertainty contributions to $\Delta\alpha$ is given in Table II.

In comparison, the atomic structure calculations of Porsev and Derevianko [15] give $\Delta\alpha = 4.305(59) \times 10^{-39}\ \mathrm{C\,m^2/V}$, a difference of more than 3σ from our value. This is still within the typical range of deviation between calculated and experimental values, e.g., lifetimes in Ref. [16].

As discussed in the introduction, for improving strontium lattice clocks to the 10^{-18} uncertainty range, the dynamic shift contribution $\Delta\nu_{\mathrm{dyn}}$ [Eq. (1)] needs to be determined. We calculated its value by first determining the ac polarizabilities $\alpha_i(\omega)$ of the clock states ($i = e, g$) (Fig. 1) using Einstein coefficients A_{ki}:

TABLE II. Uncertainty budget of measurement of the differential dc polarizability $\Delta\alpha$.

Source	Fractional contribution (10^{-6})
Separation	15.8
Voltage U	
Realization	18.5
Charging of capacitor	5.0
Inverting, drift	2.0
Residual voltage divider	0.3
Fringe and stray fields	2
Time varying bias fields	0.3
Hyperpolarizability	12
Statistical uncertainty ν, U	4.0
Total uncertainty	28

$$\alpha_i(\omega) = 2\pi\epsilon_0 c^3 \sum_k \frac{2J_k+1}{2J_i+1}\frac{A_{ki}}{\omega_{ik}^2(\omega_{ik}^2-\omega^2)}, \quad (4)$$

and then integrating the differential ac-Stark shift over the Planck distribution [26]. Here, ω_{ik} denotes the angular frequency of the transition $k \rightarrow i$ and J_i and J_k the angular momenta.

We used our measured static polarizability in combination with other observables as magic wavelength, atomic lifetimes, Thomas-Reiche-Kuhn sums [27], and ac-Stark shifts of the clock laser field [28] to adjust the A_{ki} with the largest contribution in a least squares fit (see Supplemental Material [29]). In this way we include the best experimental knowledge to improve $\Delta\nu_{\mathrm{dyn}}$.

In order to obtain an uncertainty estimation for $\Delta\nu_{\mathrm{dyn}}$, we performed 2000 fit runs to synthetic data sets, i.e., sets of observables varied at random within their respective uncertainties [30]. From the Monte Carlo simulation (see Supplemental Material [29]) we find that the dynamic BBR shifts of the two clock levels at $T_0 = 300$ K are -150.4 and -2.8 mHz for exited and ground states.

In summary, the clock transition resonance frequency is shifted by BBR of temperature T by

$$\Delta\nu(T) = \Delta\nu_{\mathrm{stat}}\left(\frac{T}{T_0}\right)^4 + \Delta\nu_{\mathrm{dyn}}\left[\left(\frac{T}{T_0}\right)^6 + \mathcal{O}\left(\frac{T}{T_0}\right)^8\right], \quad (5)$$

with $\Delta\nu_{\mathrm{stat}} = -2.13023(6)$ Hz and $\Delta\nu_{\mathrm{dyn}} = -147.6(23)$ mHz. Compared to the corrections used thus far [16] of 2.354 (32) Hz at 300 K, applying our correction shifts the clock frequency by a fraction of -1.8×10^{-16}. While this is on the order of the uncertainties of the best Sr lattice clocks, it is below the uncertainties of the measured frequencies. In the course of this work a numerical error in the calculation of the dynamic corrections in Ref. [15] was identified [31]. This error amounts to -53 mHz, while this new study changes the correction due to the static part by 118 mHz and the dynamic part by 11 mHz.

These corrections immediately apply to ^{88}Sr. To obtain the corrections for ^{87}Sr we have repeated the calculation according to Eq. (4) using published data on isotopic shift and hyperfine structure [32–37] (see Supplemental Material [29]) and using a mass scaling of the transition dipole matrix elements [38]. All published transition isotope shifts between ^{88}Sr and ^{87}Sr lie in a range of up to 150 MHz. Thus, for the calculation for lines with unknown isotope shift, a conservative estimate of 150 MHz was assumed. With these data we obtained a fractional change of $\Delta\alpha$ of -1.2×10^{-6} and of $\Delta\nu_{\mathrm{dyn}}$ of -3.4×10^{-6}. Thus the correction [Eq. (5)] also applies to ^{87}Sr well within their uncertainties.

In conclusion, a measurement of the differential dc polarizability of the strontium clock transition in combination with a model for the frequency response of the atoms to BBR enabled us to derive an improved correction of the BBR shift and estimate its uncertainty. With this study, corrected frequencies of a number of high precision measurements of the clock transition may now be calculated [10,11,13,14]. The corrected frequencies still agree well because the applied correction is smaller than typical uncertainties of realizations of the SI second by Cs clocks. Now the shift correction coefficient leads to an uncertainty of 5×10^{-18} at room temperature, where a probably achievable temperature uncertainty of 80 mK would add the same uncertainty.

To further lower the uncertainty of strontium lattice clocks, an interrogation of the atoms in a colder environment is a viable solution [26]. For example, for a 1×10^{-18} relative frequency uncertainty, at liquid nitrogen temperature only an uncertainty of the temperature of about 1 K is needed, while the shift coefficient introduces a completely negligible uncertainty.

We thank H. H. Ernst, A. Felgner, P. Franke, D. Hagedorn, R. Krüger-Sehm, F. Lechelt, A. Linkogel, and M. Schulz for valuable technical assistance and R. Zirpel for equipment loan. This work was financially supported by the European Metrology Research Programme EMRP under IND 014 and the Centre for Quantum Engineering and Space-Time Research QUEST. The EMRP is jointly funded by the EMRP participating countries within EURAMET and the European Union .

*stephan.falke@ptb.de

[1] T. Rosenband, D. B. Hume, P. O. Schmidt, C. W. Chou, A. Brusch, L. Lorini, W. H. Oskay, R. E. Drullinger, T. M. Fortier, J. E. Stalnaker *et al.*, Science **319**, 1808 (2008).
[2] Y. Y. Jiang, A. D. Ludlow, N. D. Lemke, R. W. Fox, J. A. Sherman, L.-S. Ma, and C. W. Oates, Nat. Photonics **5**, 158 (2011).
[3] M. Takamoto, T. Takano, and H. Katori, Nat. Photonics **5**, 288 (2011).
[4] C. Hagemann, C. Grebing, T. Kessler, S. Falke, C. Lisdat, H. Schnatz, F. Riehle, and U. Sterr, arXiv:1208.1634v1 [IEEE Trans. Instrum. Meas. (to be published)].

[5] E. Peik, B. Lipphardt, H. Schnatz, T. Schneider, C. Tamm, and S. G. Karshenboim, Phys. Rev. Lett. **93**, 170801 (2004).

[6] V. A. Dzuba and V. V. Flambaum, Can. J. Phys. **87**, 15 (2009).

[7] S. Blatt, A. D. Ludlow, G. K. Campbell, J. W. Thomsen, T. Zelevinsky, M. M. Boyd, J. Ye, X. Baillard, M. Fouché, R. L. Targat *et al.*, Phys. Rev. Lett. **100**, 140801 (2008).

[8] H. Katori, Nat. Phys. **5**, 203 (2011).

[9] A. Bjerhammar, Bulletin Geodesique **59**, 207 (1985).

[10] G. K. Campbell, A. D. Ludlow, S. Blatt, J. W. Thomsen, M. J. Martin, M. H. G. de Miranda, T. Zelevinsky, M. M. Boyd, J. Ye, S. A. Diddams *et al.*, Metrologia **45**, 539 (2008).

[11] S. Falke, H. Schnatz, J. S. R. Vellore Winfred, T. Middelmann, S. Vogt, S. Weyers, B. Lipphardt, G. Grosche, F. Riehle, U. Sterr *et al.*, Metrologia **48**, 399 (2011).

[12] J. A. Sherman, N. D. Lemke, N. Hinkley, M. Pizzocaro, R. W. Fox, A. D. Ludlow, and C. W. Oates, Phys. Rev. Lett. **108**, 153002 (2012).

[13] X. Baillard, M. Fouché, R. L. Targat, P. G. Westergaard, A. Lecallier, F. Chapelet, M. Abgrall, G. D. Rovera, P. Laurent, P. Rosenbusch *et al.*, Eur. Phys. J. D **48**, 11 (2008).

[14] A. Yamaguchi, M. Fujieda, M. Kumagai, H. Hachisu, S. Nagano, Y. Li, T. Ido, T. Takano, M. Takamoto, and H. Katori, Appl. Phys. Express **4**, 082203 (2011).

[15] S. G. Porsev and A. Derevianko, Phys. Rev. A **74**, 020502 (2006).

[16] S. G. Porsev, A. D. Ludlow, M. M. Boyd, and J. Ye, Phys. Rev. A **78**, 032508 (2008).

[17] E. Simon, P. Laurent, and A. Clairon, Phys. Rev. A **57**, 436 (1998).

[18] J. Robyr, P. Knowles, and A. Weis, IEEE Trans. Ultrason. Ferroelectr. Freq. Control **57**, 613 (2010).

[19] T. Middelmann, S. Falke, C. Lisdat, and U. Sterr, New J. Phys. **14**, 073020 (2012).

[20] T. Legero, C. Lisdat, J. S. R. Vellore Winfred, H. Schnatz, G. Grosche, F. Riehle, and U. Sterr, IEEE Trans. Instrum. Meas. **58**, 1252 (2009).

[21] S. Falke, M. Misera, U. Sterr, and C. Lisdat, Appl. Phys. B **107**, 301 (2012).

[22] P. Franke and R. Schödel, PTB Mitteilungen **120**, 16 (2010).

[23] C. Degenhardt, H. Stoehr, C. Lisdat, G. Wilpers, H. Schnatz, B. Lipphardt, T. Nazarova, P.-E. Pottie, U. Sterr, J. Helmcke *et al.*, Phys. Rev. A **72**, 062111 (2005).

[24] N. A. Robertson, J. R. Blackwood, S. Buchman, R. L. Byer, J. Camp, D. Gill, J. Hanson, S. Williams, and P. Zhou, Classical Quantum Gravity **23**, 2665 (2006).

[25] H. Michaelson, J. Appl. Phys. **48**, 4729 (1977).

[26] T. Middelmann, C. Lisdat, S. Falke, J. S. R. Vellore Winfred, F. Riehle, and U. Sterr, IEEE Trans. Instrum. Meas. **60**, 2550 (2011).

[27] E. U. Condon and G. H. Shortley, *The Theory of Atomic Spectra* (Cambridge University Press, Cambridge, England, 1953).

[28] X. Baillard, M. Fouché, R. L. Targat, P. G. Westergaard, A. Lecallier, Y. Le Coq, G. D. Rovera, S. Bize, and P. Lemonde, Opt. Lett. **32**, 1812 (2007).

[29] See Supplemental Material at http://link.aps.org/supplemental/10.1103/PhysRevLett.109.263004 for information about fitting parameters and results as well as possible isotope corrections.

[30] C. Degenhardt, H. Stoehr, U. Sterr, F. Riehle, and C. Lisdat, Phys. Rev. A **70**, 023414 (2004).

[31] All dynamical corrections need to be increased by 50.4%, A. Derevianko (private communication); see also S. G. Porsev and A. Derevianko, Phys. Rev. A **86**, 029904(E) (2012).

[32] A. Aspect, J. Bauche, M. Godefroid, P. Grangier, J. E. Hansen, and N. Vaeck, J. Phys. B **24**, 4077 (1991).

[33] M. Anselment, S. Chongkum, K. Bekk, S. Göring, A. Hanser, G. Meisel, and H. Rebel, Z. Phys. D **3**, 421 (1986).

[34] R. Le Targat, Ph.D. thesis, ENST, Paris, 2007 [http://tel.archives-ouvertes.fr/tel-00170038/fr].

[35] C. J. Lorenzen, K. Niemax, and L. R. Pendrill, Phys. Rev. A **28**, 2051 (1983).

[36] F. Buchinger, R. Corriveau, E. B. Ramsay, D. Berdichevsky, and D. W. L. Sprung, Phys. Rev. C **32**, 2058 (1985).

[37] E. R. Eliel, W. Hogervorst, T. Olsson, and L. R. Pendrill, Z. Phys. **311**, 1 (1983).

[38] W. L. Wiese and J. R. Fuhr, J. Phys. Chem. Ref. Data **38**, 565 (2009).